www.vbripress.com, www.amlett.com, DOI: 10.5185/amlett.2011.1206 Published online by the VBRI press in 2011

Silver nanoparticles: preparation, characterization, and kinetics

Javed Ijaz Hussain[1], Sunil Kumar[2], Athar Adil Hashmi[1], Zaheer Khan[1,3*]

[1]*Department of Chemistry, Jamia Millia Islamia (Central University), New Delhi 110025, India*
[2]*Department of Chemistry, University of Delhi, New Delhi 110007, India*
[3]*Department of Chemistry, Faculty of Science, King Abdul Aziz University, P.O. Box 80203, Jeddah 21413, Saudi Arabia*

[*]Corresponding author. Tel: (+91) 11 26981717; Fax: (+91) 11 26980229; E-mail: drkhanchem@yahoo.co.in

Received: 5 Jan 2011, Revised: 17 Feb 2011 and Accepted: 01 March 2011

ABSTRACT

In this paper we report the effect of aniline concentrations on the growth and size of silver nanocrystals using aniline and silver nitrate as reductant and oxidant, respectively. UV-Vis spectroscopy, transmission electron microscopy (TEM) and selected areas electron diffraction (SAED) have been employed to characterize silver nanoparticles. The TEM images show that silver nanocrystals are roughly spherical and of uniform particle size, and the average particle size is *ca*. 25 nm. A broad surface plasmon resonance band appears at 400 nm. The rings patterns are in good agreement with the standard values of the face-centered-cubic form of silver nanocrystals. This is attributed to the adsorption of aniline and /or interparticle interaction onto the surface of Ag-nanocrystals through electrostatic interactions between the lone-pairs electrons of $-NH_2$ and positive surface of Ag- nanoparticles.

Keywords: Nanostructures; chemical synthesis; surfaces properties; aniline.

Jawed Ijaz Hussain is a Ph.D. student in Department of Chemistry, Jamia Milia Islamia, New Delhi, India.

Athar Adil Hashmi is working as Associate Professor in the Department of Chemistry, Jamia Millia Islamia, New Delhi, India. His work area includes organometallic chemistry, metal containing polymers and bio- inorganic chemistry.

Zaheer Khan is the Professor in the Department of Chemistry, Jamia Millia Islamia, New Delhi, India. His current research interests include the synthesis, kinetics and mechanism of the advanced nano materials of silver and manganese by green routs.

Introduction

Silver nanocrystals, mostly hydrosols are one of the most attractive inorganic material not only because of its tremendous applications in photography **[1]**, catalysis **[2]**, biosensor **[3]**, biomolecular detection **[4]**, diagnostics **[5]**, and particularly antimicrobial **[6- 8]** activities but also because of its environmentally benign nature **[9-12]**. Synthesis of different morphologies of advanced silver nanomaterials (nanotubes, nanowires, nano cubes, nanorods, and nanosheets) has been the subject of a large number of researchers in many laboratories **[13-17]**. A number of methods were used in the past for the synthesis of silver nanoparticles for example, reduction in solutions **[18]**, radiation assisted **[19]** chemical and photoreduction in reverse micelles **[20]**, thermal decomposition of silver compounds **[21]** and recently via bio- or green-synthesis route **[7, 16, 22]**.

A multitude of chemical reduction methods have been applied to synthesize stable and various shapes of silver nanoparticles in water by the use of different reducing agents (ascorbic acid **[23]**, hydrazine **[24]**, ammonium formate **[25]**, dimethylformamide**[26]** and sodium borohydride **[27]**). The shape, size and the size distribution strongly depended on the strong and weak tendency of organic substrates to reduce the silver salts. Biosynthetic methods employing either biological microorganisms such as bacteria **[28]**, fungi **[29]**, yeast **[30]** or plant extracts **[31, 32]** have emerged as an alternative to chemical synthetic procedures and physical methods were well documented in

the literature. The presence of various natural products (carbohydrates, alkaloids, steroids, proteins and/or peptides) in plant extract, and the tendency of Ag ions to form a variety of complexes with carbohydrates and proteins**,** all combine to give systems of considerable complexity. The simplest and the most commonly used bulk- solution synthetic method for metal nanoparticles is the chemical reduction of metal salts. Using chemical reduction methods for synthesis of different morphologies nanoparticles can be advantageous over other biosynthetic processes because it involves reduction of an ionic salt in the presence of surfactant using a reducing agent as well as it is cost effective, easily scaled up for large-scale synthesis and further there is no need to use high pressure, energy and temperature.

Reduction of silver(I) by chemical methods proceeds through a one-step process to produce a colored silver sol because surface of a metal having free electrons in the conduction band and positively charged nuclei. Therefore, formation of long-lived clusters of silver by the chemical method (Ag^+ ions - sodium borohydride reaction in presence of polyanion) has been the reported by Henglein and his coworkers for the first time **[33,34]**.

Aniline, one of the water soluble aromatic amine, well known weak reducing agent, has an ability of one-step reduction and coordinates with silver ions. Li and his co-workers used aniline as stabilizer for controlling the morphology and particle size of Ag-nanoparticles using hydrazine and sodium citrate as the reducing agents **[35]**. In this paper, we demonstrate a simple chemical reduction aniline route for the synthesis of silver nanocrystals. Studies revealed that the reaction conditions ([CTAB] and [aniline]) content have great influence on the morphologies of silver nanoparticles. The synthetic conditions were optimized by changing the concentrations of aniline, CTAB and Ag^+ ions.

Experimental

Chemicals

CTAB, $AgNO_3$, NaCl and NaBr were the same as used earlier **[23, 35]**. Aniline (Merck, 99%) was used after purification under a stream of nitrogen gas. Doubly distilled and deionized water (specific conductance (1-2) × 10^{-6} ohm^{-1} cm^{-1}) was used as solvent for preparing the stock solutions of all reagents. Owing to the aerial oxidation of aniline in water, solutions were prepared daily, stored in amber colored glass bottle.

Kinetic method

In order to determine the rate of the silver nanoparticles formation, reactions were carried out in three-necked glass-stopper flasks fitted with a double - walled spiral condenser to arrest evaporation. Required amounts of $AgNO_3$ (oxidant), CTAB (stabilizer) and water, were introduced into the reaction vessel. The reaction was started by adding the requisite, and thermally equilibrated, solution of aniline (reductant). The progress of the reaction was followed spectrophotometrically (UV-visible Recording Spectrophotometer, UV-260 Shimadzu, with 1cm quartz cuvettes) by pipetting out aliquots at definite time intervals and measuring the absorbance of silver sol formation at 400 nm (λmax of pale-yellow color). Duplicate runs gave results that were reproducible to within ± 4 %. The apparent rate constants (k_{obs}, s^{-1}) were calculated from the initial part of the slopes of the plots of ln (a / (1 – a)) *versus* time with a fixed time method **[36]**. The pH of the reaction mixture was also measured at the beginning and end of each kinetic experiment.

Preparation and characterization of silver nanoparticles

For the preparation of silver-nanoparticles, $AgNO_3$ solution (0.01 mol dm^{-3}) and CTAB (0.01 mol dm^{-3}) were used, respectively, as a metal salt precursor and a stabilizing agent. Aniline solution (0.01 mol dm^{-3}) was also used as a reducing agent. The transparent colorless reaction mixture containing $AgNO_3$ + CTAB was converted to the characteristic pale yellow color after the addition of a required solution of aniline. The appearance of color was indicated the formation of silver nanoparticles. Transmission electron microscope (JEOL, JEM-1011; Japan) was used to determine the size, shape and the size distribution of the silver nanoparticles. Samples were prepared by placing a drop of working solution on a carbon-coated standard copper grid (300 mesh) operating at 80 kV. FT-IR experiments were carried out on a Bruker Equinox 55 spectrophotometer. Silver sol was examined as usual by conventional method using a thin KBr pellet.

Results and discussion

General considerations

The pH of a reaction mixture play an important in the preparation and synthesis of different shaped and sized nanoparticles and nanocomposites of Ag and Au ions in presence of amino acids **[37]**. Silver sol is unstable in aqueous solutions of $[H^+] > 1.0\times10^{-3}$ mol dm^{-3}. Stability of Ag- nanoparticles depends strongly on the pH of the working solutions and its growth can be stopped by adding the small amounts of minerals acids **[33]**. Therefore, control of pH is a crucial problem that we address first. The control of pH is not as straightforward in micelles solutions as in ordinary solvents **[38]**. In order to see any change in the pH during the redox process, a series of experiments were carried out in presence of [CTAB] and /or aniline. The pH values was found to be nearly constant with increasing [CTAB] and [aniline] (pH was found to be constant, i.e., 10.3 ± 0.03 at [aniline] values of 5.0 , 10.0, 20.0, 30.0 and 50.0 $\times10^{-4}$ mol dm^{-3} in presence of CTAB (10.0×10^{-4} mol dm^{-3}). It is not surprising because ionic micelles show a marked difference in the effective local pH to exist at its micellar surface over that in bulk aqueous solvent. The different pH in the micellar pseudo phase of ionic micelles is understandable because most of the ionic (acidic and basic) species should be in the micellar phase and in addition pKs in micellar systems are almost of time different from the pKs measured in water.

Preliminary observations showed that the reduction of Ag^+ ions by aniline is very slow at room temperature (33 ^{0}C), and colorless mixture becomes yellow turbid as the reaction time increases. Therefore, CTAB was used as the stabilizing agents in the present studies. In the first set of experiments, aniline solution (10 cm^3 , 0.01mol dm^{-3}) was added to a solutions containing silver nitrate (8 cm^3,

0.01mol dm^{-3}) and CTAB (= 2 -20 cm^3, 0.01mol dm^{-3}, total vol. 50 cm^3) at 33 ^oC. The most interesting feature of the present observations is the appearance of prefect transparent pale yellow color instead of yellow turbidity after the addition of aniline. The appearance of color is caused by the surface plasmon resonance of Ag-nanocrystals in the visible region **[16, 39]**. Formation of transparent silver sol was observed between $4.0\times10^{-4} \leq$ [CTAB] $\geq 14.0\times10^{-4}$ mol dm^{-3} with [Ag(I)] = 16.0×10^{-4} mol dm^{-3} and [aniline] = 20.0×10^{-4} mol dm^{-3}. At higher [CTAB] ($\geq 16.0\times10^{-4}$ mol dm^{-3}), the reaction mixture becomes turbid and a gray precipitate appears. In the second set of experiments, different volumes of silver(I) solutions in the range 1 -10 cm^3, 0.01mol dm^{-3} were added to a reaction mixture containing aniline (10 cm^3, 0.01mol dm^{-3}) and CTAB (4 cm^3, 0.01 mol dm^{-3}). Yellowish-black precipitate is formed at [$AgNO_3$] (> 5.0×10^{-3} mol dm^{-3}).

Characterization of Ag-nanocrystals

It is well known that silver nanoparticles exhibit yellowish brown color in aqueous solution due to excitation of surface plasmon resonance band in the U.V.-visible region **[39, 40]**. As the aniline solution was mixed with aqueous solution of the silver nitrate and CTAB, it started to the appearance of pale-yellow color due to reduction of silver ion; which indicated the formation of silver nanoparticles. It is generally accepted that UV–Vis spectroscopy could be used to examine size and shape-controlled nanoparticles in aqueous solution. **Fig. 1** shows the UV–Vis spectra recorded from the reaction medium after 100 min. The absorption spectra of silver sol consists a single sharp surface plasmon resonance band at 400 nm (**Fig. 1**). The most characteristic part of silver sol is a narrow plasmon absorption band observable in the 350 – 600 nm regions. A broad surface plasmon resonance band is due to aggregation and/or adsorption of aniline onto the surface of Ag-nanocrystals.

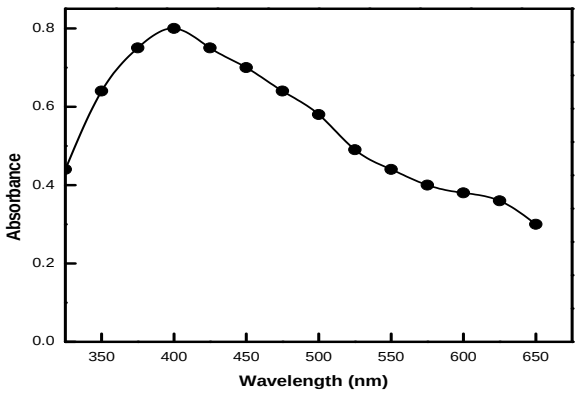

Fig. 1. Spectra of silver-nanocrystals. *Reaction conditions*: [aniline] = 40.0×10^{-4} mol dm^{-3}; [CTAB] = 10.0×10^{-4} mol dm^{-3}; [Ag^+] = 14.0×10^{-4} mol dm^{-3}.

TEM images of silver sol are shown in **Fig. 2**. These observations indicate the adsorption and/or deposition of silver nanoparticles onto the surface of roughly sphere-shaped polydispersed particles for [Ag^+] / [aniline] ratios of 0.8, 0.4 and 0.3, respectively. The Ag-nanocrystals that emerged in the images have variety of shapes: spherical, triangle and irregular. As can be seen in **Fig. 2 (D)** (typical example), presence of rings patterns in the selected area electron diffraction reveals the single face-centered cubic (fcc) crystalline nature of the spherical nanoparticles with a preferential growth direction along the Ag (110), (200), (220), (311) and (331) planes. In agreement with the U. V.-vis spectrophotometric observations, the TEM images reveal Ag-nanocrystals are polydisperse, irregular deposition and roughly spherical of a rather similar diameter 25 nm. Our results are quite consistent with that of Guzman et al. **[7]** for the synthesis of silver nanoparticles by chemical reduction method and their antibacterial activity. Goia and Matijevic **[41]** and El-Sayed et al. **[42]** suggested that faceted or rodlike nanoparticles are formed during the reduction of metal salts by weak reducing agents where growth occurs over a longer period.

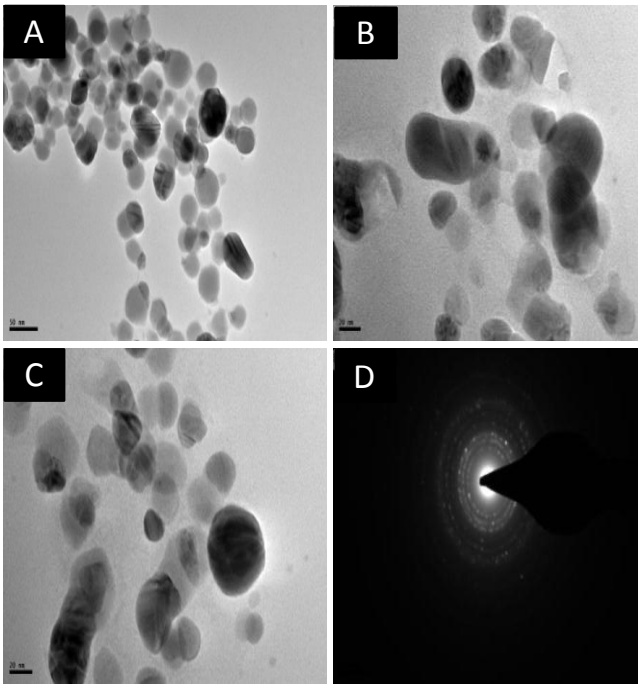

Fig. 2. TEM images of Ag-nanocrystals. *Reaction conditions*: [CTAB] = 10.0×10^{-4} mol dm^{-3}; [Ag^+] / [aniline] = 0.7 (A), 0.35 (B) and 0.28 (C). Selected area diffraction images of randomly selected Ag-nanocrystals (D).

Effect of [Ag^+ ions], [aniline] and mechanism of Ag-nanocrystals

The dependence of the silver sol formation kinetics on the [Ag^+] was studied between $2.0\times10^{-4} \leq$ [$AgNO_3$] $\geq 30.0\times10^{-4}$ mol dm^{-3} at fixed [CTAB] = 10.0×10^{-4} mol dm^{-3}, [aniline] = 40.0×10^{-4} mol dm^{-3}, and temperature = 33 ^0C. No silver sol formation was observed at [$AgNO_3$] = 2.0×10^{-4} mol dm^{-3}. Kinetic determinations at higher [$AgNO_3$] ($\geq 35.0\times10^{-4}$ mol dm^{-3}) were hampered due to the formation of gray precipitate. The absorbance at 400 nm *versus* time plots (**Fig. 3**) suggests that autocatalysis is involved in the silver sol formation. It was noted that the extent of induction period (nucleation) depends on the [Ag^+]. On the other hand, the absorbance-[$AgNO_3$] profiles (**Fig. 4**) show sigmoid dependence of the silver sol formation on [$AgNO_3$] establishing the autocatalytic path

involved in the formation of perfect transparent silver sol. Thus, we concluded that the aniline-Ag^+ reaction has nucleation, growth and autocatalytic reaction paths (autocatalysis is due to the formation of metal nucleation center which acts as an catalyst for the reduction of other Ag^+ present in solution).

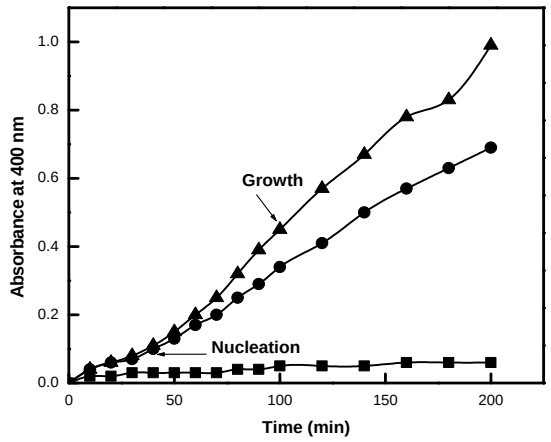

Fig. 3. Plots showing the effects of [Ag^+] on the absorbance of silver nanocrystals. *Reaction conditions*: [aniline] = 40.0 $\times 10^{-4}$ mol dm^{-3}; [CTAB] = 10.0 $\times 10^{-4}$ mol dm^{-3}; Temperature = 33 ^{0}C; [Ag^+] = 4.0 (■), 20.0 (●) and 30.0 $\times 10^{-4}$ mol dm^{-3}(▲).

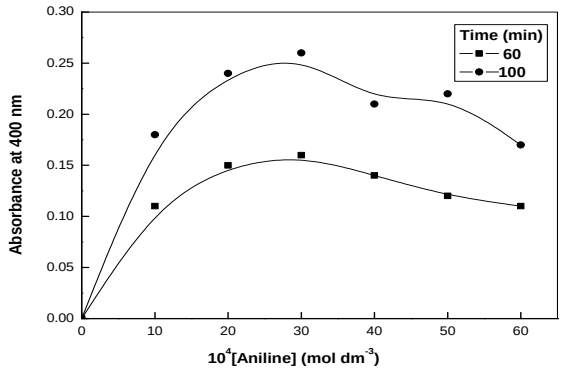

Fig. 4. Effects of [aniline] on the surface plasmon absorbance of silver sol formation at different time intervals. *Reaction conditions:* [Ag^+] = 16.0 $\times 10^{-4}$ mol dm^{-3}, [CTAB] = 10.0 $\times 10^{-4}$ mol dm^{-3}, Temperature = 33 ^{0}C. Time 60 (■) and 100 min (♦).

The effect of aniline concentrations was also studied in order to see the formation of transparent silver sol. The observed results are depicted in **Fig. 5** as absorbance-[aniline] profiles. Interestingly, the absorbance increases with the [aniline] and until it reaches a maximum then decreases with [aniline]. The increase-decrease behavior (hypo chromic shift) of absorbance after a definite time interval (**Fig. 5**) may be explained in terms of adsorption of aniline onto the surface of metallic silver particles. As a results, increases the Fermi level of particles, which in turn, increases the size, polydispersity, and the size distribution of the Ag-nanoparticles [**34**]. Henglein and his coworkers monitored the stepwise growth of silver clusters by spectroscopic methods in the presence of polymers due to the generation of hydrated electrons in pulse radiolysis or by 308 nm laser pulses and reported the mechanism of the reduction of Ag^+ ions and the association of Ag^0 atoms to produce metallic colloidal Ag particles **[33, 34, 43]**. All these considerations, along with the above observed results, lead to the proposal of the following mechanism for the formation of silver nanoparticles.

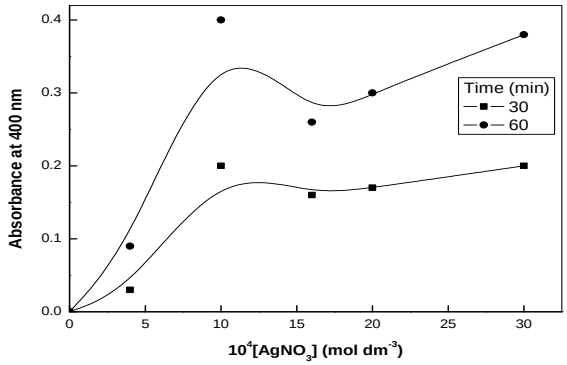

Fig. 5. Effects of [$AgNO_3$] on the surface plasmon absorbance of silver sol formation at different time intervals. *Reaction conditions:* [aniline] = 40.0 $\times 10^{-4}$ mol dm^{-3}, [CTAB] = 10.0 $\times 10^{-4}$ mol dm^{-3}, Temperature = 33 ^{0}C. Time 30 (■) and 60 min (♦).

In **Scheme 1**, Eq. 1 represents the formation of aniline-Ag complex. In the rate-determining step (Eq. 2) we assume that complex decomposes in a one step one-electron oxidation reduction mechanism to Ag^0 and radical. In the next step, the complexation of the formed Ag^0 atoms with Ag^+ ions yields Ag_2^+ ions (Eq.3), and then the Ag_2^+ ions dimerize to yield Ag_4^{2+} (Eq. 4). The proposed mechanism is further supported by the detection of radical with acrylonitrile **[44]**. Radical converted into the stable oxidation products of aniline, i.e., azobenzene after the dimerization and oxidation by available Ag^+ ions (Eq. 5).

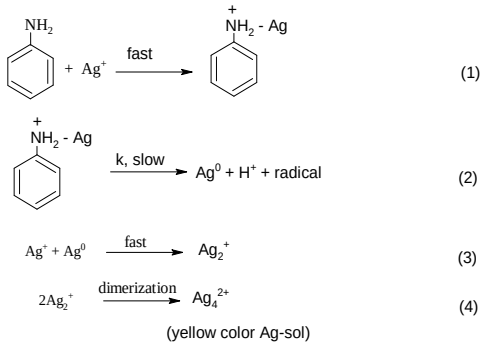

Scheme 1. Mechanism to the formation of Ag-nanoparticles

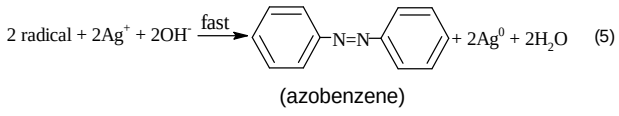

The Fourier transform infrared (FT-IR) spectra experiments were carried out on a Bruker Equinox 55

spectrophotometer. A few drops of the resulting sol were placed on a KBr pellets and allowed to dry IR spectra recorded. The nature of azobenzene as the oxidation product was confirmed by comparison its FT-IR spectra against an authentic sample of azobenzene.

A rate law consistent with Scheme 1 may be expressed as Eq.6.

$$\frac{d[\text{Ag-sol}]}{dt} = k\,[Ag^+]\,[\text{aniline}] \qquad (6)$$

Role of aniline and reaction site to the growth of Ag-nanocrystals

Micelles can stabilize the substrates, intermediates or products through hydrophobic, electrostatic, hydrogen bonding and van der Walls forces **[45]**. As a result, various properties such as oxidation-reduction potentials, dissociation-ionization constants, quantum efficiencies, reaction mechanisms, size, and shape of inorganic nanocrystals are changed. In the present study, role of CTAB can be explained by incorporation, and/or solubilization of aniline aniline- Ag^+ complex and/or silver nanoparticles onto the surface of CTAB micelles. Various properties such as oxidation-reduction potentials, dissociation-ionization constants, size, and shape of inorganic nanocrystals are changed in presence of micelles forming surfactants. Aniline may be assumed to be totally present in the Stern layer of cationic CTAB micelles due to the ion-pair formation between the positive head group ($-N^+(CH_3)_3$) and lone-pairs of $-NH_2$ group of aniline. On the other hand, the presence of non-polar phenyl group is responsible to the solubilization of aniline into the micellar palisade layer (a few carbon atoms deep toward core) hydrophobically. Amino group has strong tendency to coordinate with Ag^+. Therefore, penetration of Ag^+ into the Stern layer takes place which allows them to form complex with aniline (**Scheme 2**).

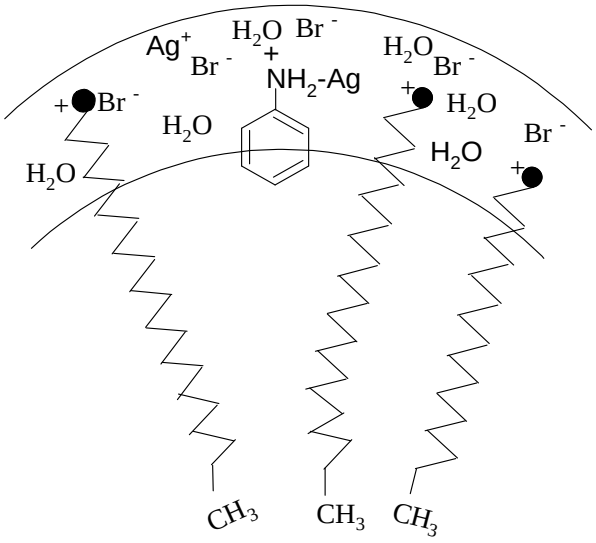

Scheme 2. Solubilization of Aniline-Ag complex into the cationic micelles of CTAB

Table 1. Values of reduction potentials (E_0), nature, pH and rate constants for the reactivity of different reductants towards Ag^+ ions in presence of CTAB.

Reductants[a]	E_0 (V)	Shape/ nature	pH /media	$10^2 k^{II}$ (mol^{-1} dm^3 s^{-1})	Ref.
Ascorbic acid	0.03	monodispersed	5.5	19.1	[23]
Cysteine	0.14	cross-linking	5.4	3.1	[35]
Hydrazine	0.23	monodispresed	7.7	0.2	[24]
Aniline	0.45	aggregation	10.3	25.0	present work
Paracetamol	0.70	polydispersed	NaOH	55.8	[46]

[a][CTAB] = 6.0 $\times 10^{-4}$ mol dm^{-3}; [reductant] = 12.0 $\times$ 10^{-4} mol dm^{-3} and [aniline] = 10.0 $\times$ 10^{-4} mol dm^{-3}; $[Ag^+]$ = 4.0, 16.0, and 6.0 $\times 10^{-4}$ mol dm^{-3} for cysteine, aniline and others, respectively; [NaOH] = 4.0 $\times$ 10^{-4} mol dm^{-3}.

It is well known that nature of reducing agents (reduction potential, E_0) is an important factor, control the size, shape and the size distribution of the Ag-nanoparticles. In order to compare the reactivity of Ag^+ ions reduction with other organic reductants, values of second-order rate constant are summarized in **Table 1**. Interestingly, the reactivity of paracetamol towards Ag^+ ions is much higher than the corresponding oxidation of many other organic substrates (**Table 1**), although it is a weaker reducing agent. Comparison of the second-order rate constants (k^{II}) shows that the reactivity decreases in the order paracetamol > aniline > ascorbic acid > cysteine > hydrazine (caution: one should keep in mind the reaction conditions; pH, temperature, etc.). This is not very surprising judging from the fact that presence of OH^- ions in the form of NaOH is responsible for the higher pH of the reaction mixture. As a result, paracetamol easily transfer the proton to Ag^+ ions leading to the formation of Ag^0. It can now be stated confidently that the pH of the working media is particularly important along with the E_0.

Conclusion

In summary, it is shown that aniline is a remarkably powerful reductant for Ag^+ ions in presence of CTAB. Mechanism, rate-law, probable reaction site and selected area electron diffraction were discussed for the first time to the preparation of monodisperse and aggregated roughly spherical Ag- nanocrystals by simple chemical reduction method. The nanoparticles formation (pale yellow color) was monitored by recording the temporal course of their absorption spectra. The single-crystallinity of Ag-nanoparticles was also confirmed by the electron diffraction patterns. It is found that shape and size distribution of the Ag-nanoparticles strongly depend on the reduction potential of the reductant and pH of the reaction media. Further progress in this area will provide green paths in the synthesis of controlled shape and size of Ag-nanoparticles as well as to speed up the removal of contaminants.

Reference

1. Albrecht, M. A.; Evans, C. W.; Raston, C. L. *Green Chem.* **2006**, *8* , 417. **DOI:** 10.1039/B517131H
2. Sun, T.; Seff, K. *Chem. Rev*. **1994**, *94*, 857. **DOI:** 10.1021/cr00028a001
3. Xiong, D. J.; Chen, M. L.; Li, H. *Chem. Commun.* **2008**, 880. **DOI:** 10.1039/B716270G
4. Duran, N.; Marcato, P. D. ; Alves, O. L. ; De Souza, G. I. H. ; Esposito, E. *J. Nanobiotechnology*. **2005**, *3*, 8. **DOI:** 10.1186/1477-3155-3-8

5. Basu, S.; Jana, S.; Pande, S. ; Pal, T. *J. Colloid and Interface Sci.* **2008,** *321*, 288. **DOI:** 10.1016/j.jcis.2008.02.015
6. Brigger, I. ; Dubernet, C. ; Couvreur, P. *Adv. Drug. Deliv. Rev.* **2004**, *54*, 631. **DOI:** 10.1016/S0169-409X(02)00044-3
7. Guzman, M. G.; Dille, J.; Godet, S.*World Acad. Sci. Eng. Technolo.* **2008**, *43*, 357.
8. Zhu, Z. ; Kai, L.; Wang, Y. *Mater. Chem. Phys.* **2006**, *96*, 447. **DOI:** 10.1016/j.matchemphys.2005.07.067
9. Sondi, I. ; Salopek-Sondi, B. *J. Colloid Interface Sci.* **2004** , *275*, 177. **DOI:** 10.1016/j.jcis.2004.02.012
10. Yu, D.; Yam, V. W.-W. *J. Am. Chem. Soc.* **2004**, *126*, 13200. **DOI:** 10.1021/ja046037r
11. Harada, M. ; Inada, Y.; Nomura, M. *J. Colloid Interface Sci.* **2009,** *337*, 427. **DOI:** 10.1016/j.jcis.2009.05.035
12. Dubas, S. T.; Pimpan, V. *Talanta*, **2008**, *76*, 29. **DOI:** 10.1016/j.talanta.2008.01.062
13. Mulvaney, P.; Wilson, O. ; Wilson, G. I. *Adv. Mater.* **2002**, *14*, 1000. **DOI:** 10.1002/1521-4095(20020705)14:13/14<1000::AID-ADMA1000>3.0.CO;2-E.
14. Tan, Y. ; Li, Y. ; Zhu, D. *J. Colloid Interface Sci.* **2003,** *258* , 244. **DOI:** 10.1016/S0021-9797(02)00151-0
15. Yu, D.; Yam, V. W.-W. *J. Phys. Chem. B*, **2005**, *109* , 5497. **DOI:** 10.1021/jp0448346
16. Xie, J.; Lee, J. Y.; Wang, D. I. C. ; Ting, Y. P. *ACS Nano*, **2007**, *1* , 429. **DOI:** 10.1021/nn7000883
17. Kim, M. ; Byun, J.-W. ; Shin, D.-S. ; Lee, Y.-S. *Mat. Res. Bull.* **2009,** *44*, 334. **DOI:** 10.1016/j.materresbull.2008.05.014
18. Taleb, C. ; Petit, M. ; Pileni, P. *Chem. Mater.* **1997**, *9* , 950. **DOI:** 10.1021/cm960513y
19. Henglein, A. *Langmuir* **2001,** *17*, 2329. **DOI:** 10.1021/la001081f
20. Esumi, K. ; Tano, T. ; Torigoe, K. ; Meguro, K. *Chem. Mater.* **1990**, *2*, 564. **DOI:** 10.1021/cm00011a019
21. Zhu, J.J.; Liu, S.W. ; Palchik, O.; Koltypin, Y.; Gedanken, A. *Langmuir* **2000**, *16*, 6396. **DOI:** 10.1021/la991507u
22. Sharma, V. K.; Yngard, R. A.; Lin, Y. *Ads. Colloid Interface Sci.* **2009,** *145*, 83. **DOI:** 10.1016/j.cis.2008.09.002
23. Al-Thabaiti, S. A.; Al- Nawaiser, F. M. ; Obaid, A. Y.; Al- Youbi, A. O.; Khan, Z. *Colloids Surfs. B: Biointerfaces* **2008,** *67*, 230. **DOI:** 10.1016/j.colsurfb.2008.08.022
24. Khan, Z.; Al- Thabaiti, S .A.; El- Mossalamy, E .H.; Obaid, A .Y. *Colloids Surf B: Biointerfaces* **2009**, *73*, 284. **DOI:** 10.1016/j.colsurfb.2009.05.030
25. Won, H. II; Nersisyan, H.; Won, C. W. ; Lee, J.-M. , Hwang, J.-S. *Chem. Eng. J.* **2010,** *156* , 459. **DOI:** 10.1016/j.cej.2009.10.053
26. Pastoriza, I.; Liz-marzan, L. M. *Pure Appl. Chem.* **2000**, *72*, 83. **DOI:** 10.1351/pac200072010083
27. Solomon, S. D. ; Bahadory, M.; Jeyarajasingam, A. V.; Rutkowsky, S. A.; Boritz, C. *J. Chem. Edu.* **2007**, *84*, 322. **DOI:** 10.1021/ed084p322
28. Saifuddin, N. ; Wong, C. W.; Nur, A. A.; Yasumira, *Eur. J. Chem.* **2009**, *6*, 61 **DOI:** 10.1007/978-3-642-18312-6_2
29. Duran, N.; Marcato, P. D. ; De Souza, G. I. H.; Alves, O.L.; Esposito, E. *J. Biomed. Nanotechnol.* **2007**, *3*, 203. **DOI:** 10.1166/jbn.2007.022
30. Kowshik, M.; Ashtaputre, S.; Kharraz, S. ; Vogel, W. ; J. ; Kulkarni, S.K.; Paknikar, K.M. *Nanotechnology* **2003**, *14*, 95. **DOI:** 10.1088/0957-4484/14/1/321
31. Haverkamp, R.G.; Marshall, A.T. *J. Nanoparticle Res.* **2009**, *11*, 1453. **DOI:** 10.1007/s11051-008-9533-6
32. Shankar, S.S.; Ahmad, A.; Pasricha, R. ; Khan, M. I.; Kumar, R. ; Sastry, M.; *J . Colloid Interface Sci.* **2004,** *274*, 69. **DOI:** 10.1016/j.jcis.2003.12.011
33. Linnert, T.; Mulvaney, P.; Henglein, A. *J. Am. Chem. Soc.* **1990,** *112*, 4657. **DOI:** 10.1021/ja00168a005
34. Henglein, A. *J. Phys. Chem.* **1993,** *97*, 5457. **DOI:** 10.1021/j100123a004
35. Khan, Z. ; Talib, A. *Colloid and Surf. B: Biointerfaces* **2010**, *76*, 164. **DOI:** 10.1016/j.colsurfb.2009.10.029
36. Huang, Z.-Y. ; Mills, G.; Hajek, B. *J. Phys. Chem.* **1993**, *97*, 11542. **DOI:** 10.1021/j100146a031
37. Dey, G. R.; Kishore, K. *Radiat. Phys. Chem.* **2005,** *72* , 565. **DOI:**10.1016/j.radphyschem.2004.04.027
38. Tondre, C . ; Hebrant, M. *J. Mol. Liq.* **1997,** *72*, 279. **DOI:** 10.1016/S0167-7322(97)00042-1
39. Burda, C. ; Chen, X.; Narayanan, R.; El-Sayed, M. A. *Chem. Rev.* **2005**, *105*, 1025. **DOI:** 10.1021/cr030063a
40. Liz-Marzan, L. M. *Langmuir* **2006**, *22*, 32 **DOI:** 10.1021/la0513353
41. Goia, D. V.; Matijevic, E. *New J. Chem.* **1998**, *22*, 1203. **DOI:** 10.1039/A709236I
42. Petroski, J. M.; Wang, Z. L.; Green, T. C.; El-Sayed, M. A. *J. phys. Chem. B* **1998**, *102*, 3316. **DOI:** 10.1021/jp981030f
43. Ershov, B.G. ; Henglein, A. *J. Phys. Chem. B* **1998**, *102*, 10663. **DOI:** 10.1021/jp981906i
44. Singnorella, S.; Rizzotto, M. ; Daier, V.; Frascaroli, M. I.; Palopoli, C.; Martino, D.; Bousseksou, A.; Sala, L. F. *J. Chem. Soc. Dalton Trans.* **1996,** 1607. **DOI:** 10.1039/DT9960001607
45. Tascioglu, S. *Tetrahedron* **1996**, *52*, 11113. **DOI:** 10.1016/0040-4020(96)00669-2
46. Ahmad, N.; Malik, M. A.; Al-Nowaiser, F.M.; Khan, Z. *Colloids Surfs.B: Biointerfaces* **2010**, *78*, 109. **DOI:** 10.1016/j.colsurfb.2010.02.020

